JOURNAL OF MATERIALS SCIENCE 22 (1987) 2221–2228

Morphological development on alkali halide surfaces during evaporation

Z. A. MUNIR
Division of Materials Science and Engineering, College of Engineering, University of California, Davis, California 95616, USA

The sequential changes of the surface morphology of evaporated alkali halide crystals were investigated. The origin of surface features and their dependence on temperature are described for cleaved (1 0 0) surfaces evaporated in vacuum. Qualitative and quantitative determinations of the velocity of atomic steps during evaporation were made through the use of the gold double decoration technique. The results are related to theoretical expectations and compared to previous studies.

1. Introduction

According to the terrace-ledge-kink (TLK) model [1], evaporation from a vicinal surface takes place in a sequence of steps each representing a net decrease in the total bonding energy of the evaporating species. The process is typically described as one which starts with the disconnection of an atom (ion) from a kink position in an atomic ledge (step) followed by the motion of the atom along the ledge, and subsequently its detachment from the ledge to an adsorbed position on an adjacent terrace. The final step in the evaporation process is the desorption of the adatom to the vapour. Furthermore, in accordance with the TLK model, ledges, which act as sources of adatoms, are generated at the edges of the evaporating crystal. However, steps can also be generated by dislocations, as has been described earlier by Burton *et al.* [2]. The intersection of a screw dislocation line with the evaporating surface provides a continuous source of steps while, in contrast, the intersection of edge dislocations provides steps through the repeated nucleation of two-dimensional vacancy clusters or disc-shaped holes (DSH). The prevalence of dislocation-related steps, and hence their relative contributions to the evaporation process depends principally on temperature, although other factors can make significant contributions as will be discussed in a later section.

The evaporation of alkali halides has been extensively studied in our own laboratory as well as in other institutions. This paper focuses on the morphological developments of cleaved surfaces of alkali halide crystals during evaporation. Surface topography is made visible by the gold decoration technique [3] as has been described in detail in previous publications [4, 5]. Changes in the topography over a given period of evaporation is made discernible by a double decoration technique [5, 6] in which surface features are decorated at the beginning and end of the evaporation. The bulk of the work described here was done on high purity single crystals of sodium chloride obtained from the Crystal Growth Laboratory at the University of Utah. The crystals contained the following major cation impurities with their levels indicated in parts per million (ppm): aluminium, 2; barium, 10; calcium, 3; caesium, 8; and potassium, 7.

2. Morphology of cleaved surfaces

The features described in this work are those obtained on cleaved (1 0 0) surfaces. Because of the hygroscopic nature of alkali halide crystals, evaporation studies are usually conducted on surfaces produced by cleaving the crystals in vacuum (typically $\sim 10\,\mu$Pa). The surface features produced during the cleaving process are either steps or sources of steps and hence play a dominant role in the initial phases of evaporation. Typically, vacuum cleaved (1 0 0) surfaces contain two types of features: elementary and gross cleavage steps. Examples of these features are shown in Figs 1a and b, respectively. Gross steps are multi-layered, often irregular vertical displacements while the elementary steps are simple, one atomic layer high displacements. The intersection of a cleavage step with a slip step gives rise to a V-shaped geometry as shown in Fig. 2 [7], and the intersection of an elementary step with a slip plane causes a displacement of the latter, the magnitude of which is dependent on the height of the step. The displacement of the slip plane as it crosses a multi-layered step is clearly visible in Fig. 3. The height of each monatomic step can be calculated from the measured displacement of the slip plane as it crosses a determined number of steps as has been determined in previous work [4].

When alkali halides crystals are cleaved in air, the resulting surface step morphology is markedly different as seen in Fig. 4. Water molecules adsorbed at steps cause a dissolution and a subsequent crystallization of the steps as the crystal is placed in vacuum.

3. Morphology of evaporated surfaces

3.1. Low temperature evaporation

During evaporation at low temperatures (e.g. $\lesssim 600$ K for NaCl), steps resulting from the cleavage process provide the flux for adatoms on the adjacent terraces and thus continued evaporation results in the motion

0022–2461/87 $03.00 + .12

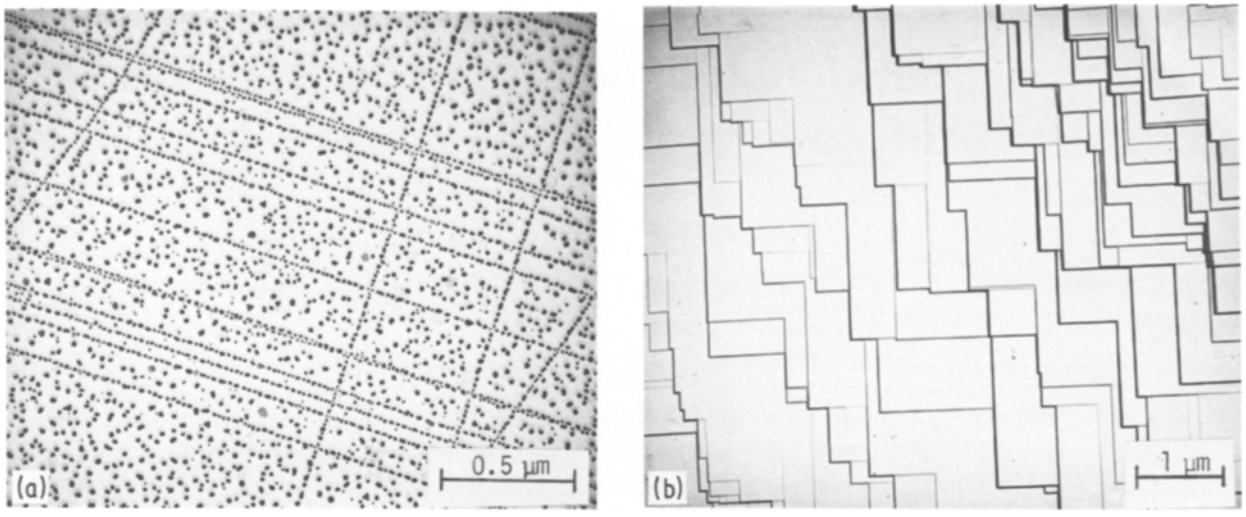

Figure 1 (a) Elementary cleavage steps on a (1 0 0) surface of NaCl. (b) Gross cleavage steps on a (1 0 0) surface of NaCl.

and subsequent disappearance of the elementary cleavage steps. Gross steps, on the other hand, prevail for longer periods of time during which they continue to generate simple steps as seen in Fig. 5.

Another source of adatoms during low temperature evaporation is the process of nucleation and growth of surface vacancy clusters, often referred to as Lochkeime or, as in this paper, disc-shaped holes (DSH). The nucleation of the DSHs is believed to be enhanced by the presence of surface impurities and is dependent on the local concentration of adatoms [8]. Bethge [8] had demonstrated the latter dependence by measuring the densities of DSHs as a function of distance from a step. Since steps are sources of adatoms, DHSs are not likely to nucleate near them as has been shown in the work referred to above [8]. As evaporation proceeds, existing DSHs grow and new ones continue to nucleate. Fig. 6 shows DSHs on a (1 0 0) surface of NaCl at different stages of growth, with some having been incorporated into existing cleavage steps. Fig. 7 is a double decoration record of a (1 0 0) NaCl surface which had been evaporated at 583 K for 4 min between decorations. During this time interval, DSHs existing before the first decoration grew as seen by the spacial changes in their perimeters (arrow A in Fig. 7). Although they can be one or two atomic planes high (i.e. $a_0/2$ or a_0 high, with a_0 being the lattice parameter for NaCl), DSHs initially nucleate in a square geometry with the sides being parallel to $\langle 1\,0\,0 \rangle$ directions. As the $a_0/2$ high DSHs grow, they become more circular in shape as seen by the example in Fig. 7 (arrow B).

3.2. Evaporation at intermediate temperatures

As the temperature of evaporation increases, marked changes take place on the evaporating surfaces. For example, in the case of NaCl evaporation over the approximate temperature range $600 < T < 735$ K is dominated by dislocation-generated steps. Screw dislocations whose lines interest the (1 0 0) surface produce steps in the form of spirals. Circular spirals are formed around the point of emergence of an $a_0/2$ [1 1 0] screw dislocation and hence have a step height of $a_0/2$. Square spirals form around the point of emergence of an a_0 [1 0 0] screw dislocation and thus have a step height of a_0. Examples of screw dislocation-generated spirals are shown in Fig. 8. Occasionally double spirals are observed on evaporated surfaces (Fig. 9). These represent the splitting of an a_0 [1 0 0] square

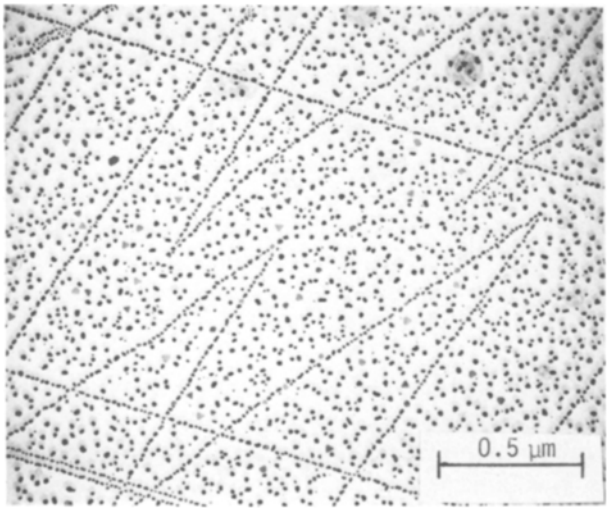

Figure 2 V-shaped elementary cleavage steps on NaCl.

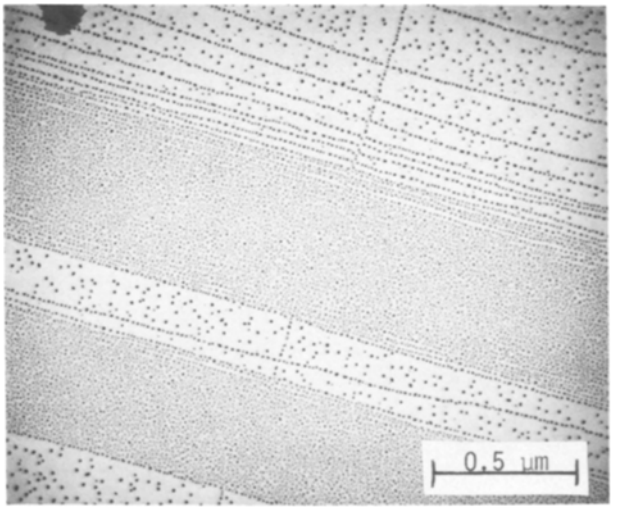

Figure 3 The displacement of a slip plane upon crossing a multilayered cleavage step.

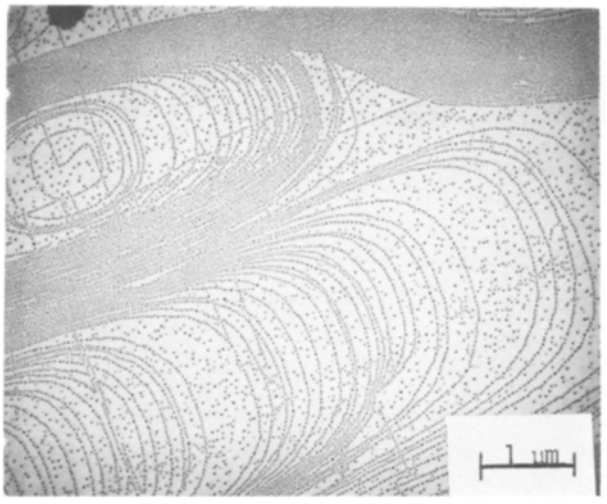

Figure 4 Morphology of air-cleaved (1 0 0) surfaces of NaCl.

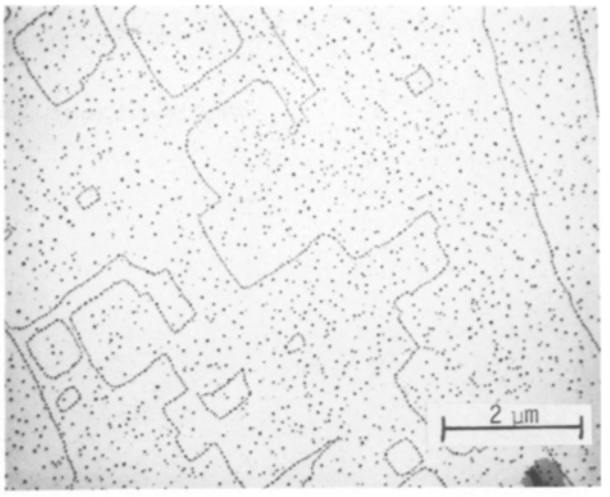

Figure 6 DSHs at different stages of growth and incorporation with evaporation steps.

spiral to form two dislocations according to: a_0 $[1\,0\,0] = a_0/2\,[1\,\bar{1}\,0] + a_0/2\,[1\,1\,0]$.

Edge dislocations generate steps through the repeated nucleation of DSHs, forming concentric round loops with a step height of $a_0/2$ or concentric square loops with a step height of a_0. The latter type is a relatively uncommon feature while the former type is relatively common on evaporated surface in this temperature range, see Fig. 10. As pointed out earlier, the morphology of surfaces evaporated in this temperature range is dominated by dislocation-generated lamellae. The extent of surface coverage of each lamella depends on the dislocation density of the sample as well as on the duration of evaporation. An evaporation lamella generated by one dislocation can cover an area as large as $400\,\mu m^2$ [6]. The relative contribution of screw dislocation lamellae to those generated by edge dislocations in the evaporation from (1 0 0) surfaces of NaCl is temperature dependent. The ratio of spirals to closed loop structures decreases with increasing temperature, as has been qualitatively observed by Vlasak [9] and quantitatively determined in recent studies by Munir *et al.* [4] and Durusoy [10]. The temperature dependence of the densities of screw and edge dislocations (exclusive of those generated at low angle tilt grain boundary) is shown in Fig. 11. For both types of dislocations the density of evaporation lamellae decreases with increasing temperature; however, the rate of decrease of screw dislocation generated lamellae (i.e. spirals) is markedly higher. At 623 K, spirals constitute about two thirds of the total evaporation lamellae while at 723 K spirals are only about one fourth of the total. The latter temperature is near the approximate upper limit where dislocation related evaporation lamellae are discernible. As will be discussed in a later section, at higher temperatures the surface features of evaporated crystals are dominated by large thermal pits [11].

In addition to isolated dislocations, low angle grain boundaries are sources of steps providing a string of edge or screw dislocations depending on whether the boundary is of the tilt or twist type, respectively. An example of a low angle tilt boundary is shown in Fig. 12a and an example of a twist boundary is shown in Fig. 12b. The interaction between dislocation-generated evaporation steps is governed by the nature of the dislocations and by the height of the steps.

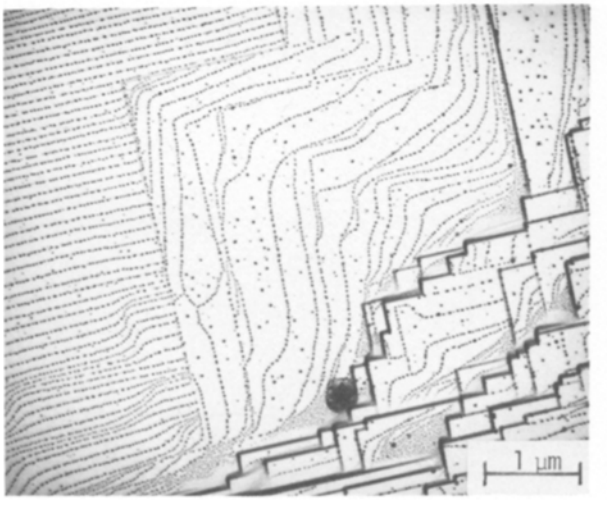

Figure 5 Generation of simple evaporation steps from gross cleavage steps.

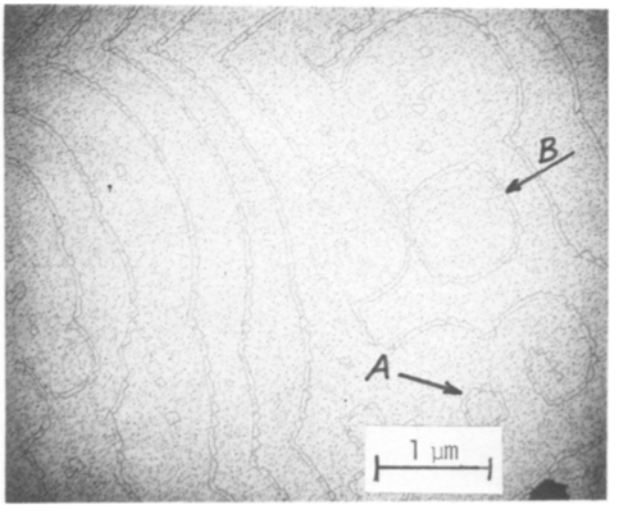

Figure 7 Growth of DSHs as seen through the double decoration technique.

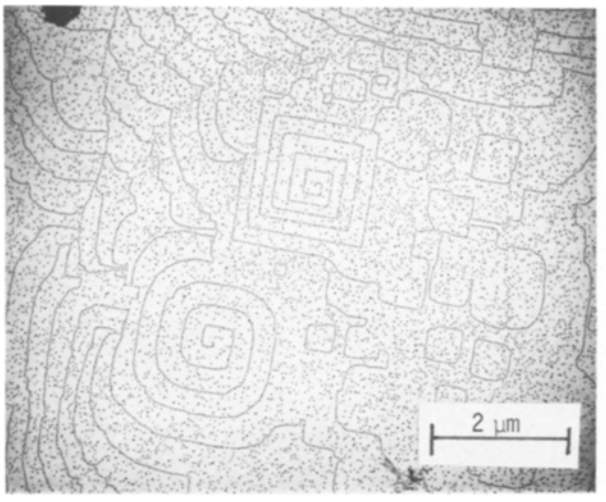

Figure 8 Square and round spirals generated by a_0 [1 0 0] and $a_0/2$ [1 1 0] screw dislocations, respectively.

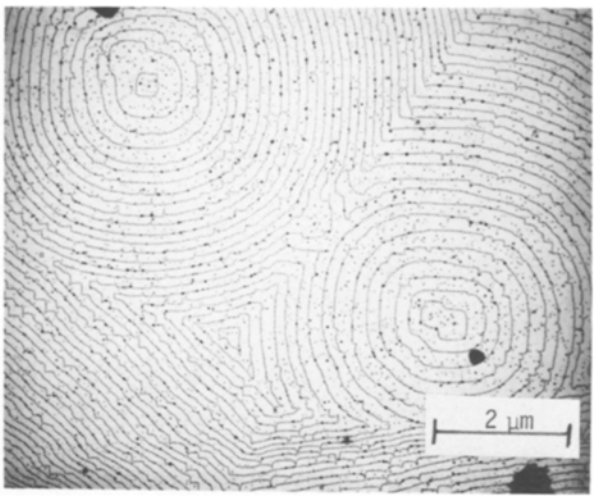

Figure 10 Concentric evaporation loops generated by edge dislocations in NaCl.

Fig. 13 shows the interaction between round steps ($a_0/2$ high) of a screw dislocation and the square steps (a_0 high) of another screw dislocation. The square (a_0 high) steps split into two $a_0/2$ high steps as the two types of lamella meet, as seen in Fig. 13. When screw dislocations having the same twist direction interact, they continue the production of spirals as seen in Fig. 14a. However, when screw dislocations with the opposite twist directions interact, concentric loops are produced as seen in Fig. 14b.

The distance between neighbouring steps in an evaporation lamella, i.e. the step separation λ, was measured for single round, double round, and square spirals [4]. Consistent with earlier observations by Keller [12], λ decreased with increasing temperature for all cases listed above. Furthermore, the spacing of square (a_0 high) spiral steps is significantly lower than the corresponding value for single round spirals [4]. The larger Burger's vector of the square spiral a_0 [1 0 0] provides a higher driving force for strain energy removal and hence a higher source frequency and a lower λ [13].

3.3. Evaporation at high temperatures

Surfaces of alkali halides evaporated at relatively high temperatures (> 750 K for NaCl) are dominated by deep (multi-layered) thermal etch pits as seen in Figs 15a and b. Fig. 15a shows the initial stage of pit formation on a (1 0 0) surface of NaCl evaporated in vacuum at 763 K for 30 min. At higher temperatures and for longer periods of evaporation, large and irregular pits form as seen in Fig. 15b which represents a (1 0 0) surface of KCl evaporated at 793 K for 120 min in vacuum. Although pit formation on evaporated surfaces of alkali halides has been examined by various investigators [11, 14, 15], agreement regarding the nature of the nucleation sites for pits is not at

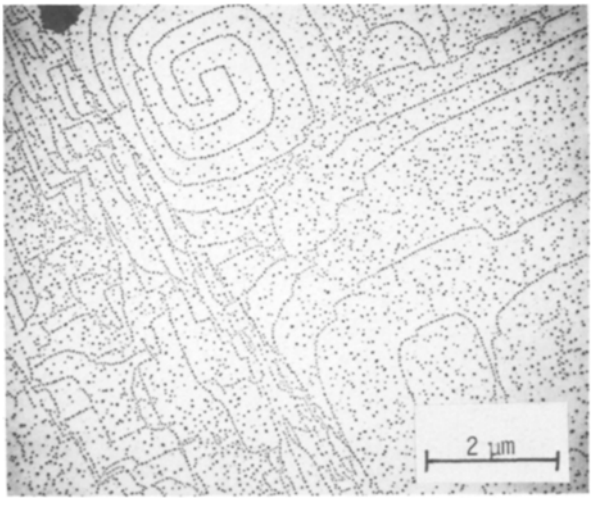

Figure 9 Double spiral on evaporated (1 0 0) surface of NaCl.

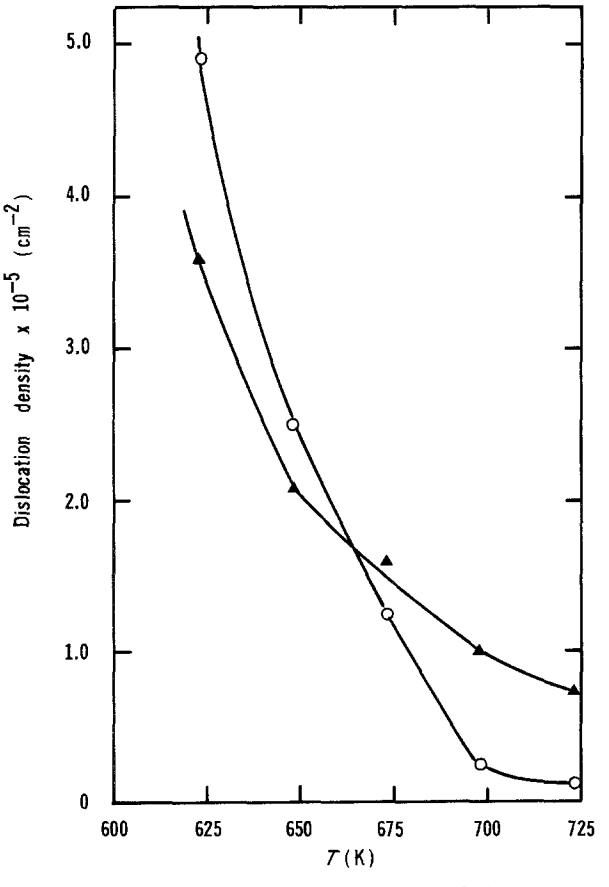

Figure 11 Temperature dependence of the density of edge and screw dislocation generated evaporation lamellae. ○, Screw dislocations; ▲, edge dislocations (average values).

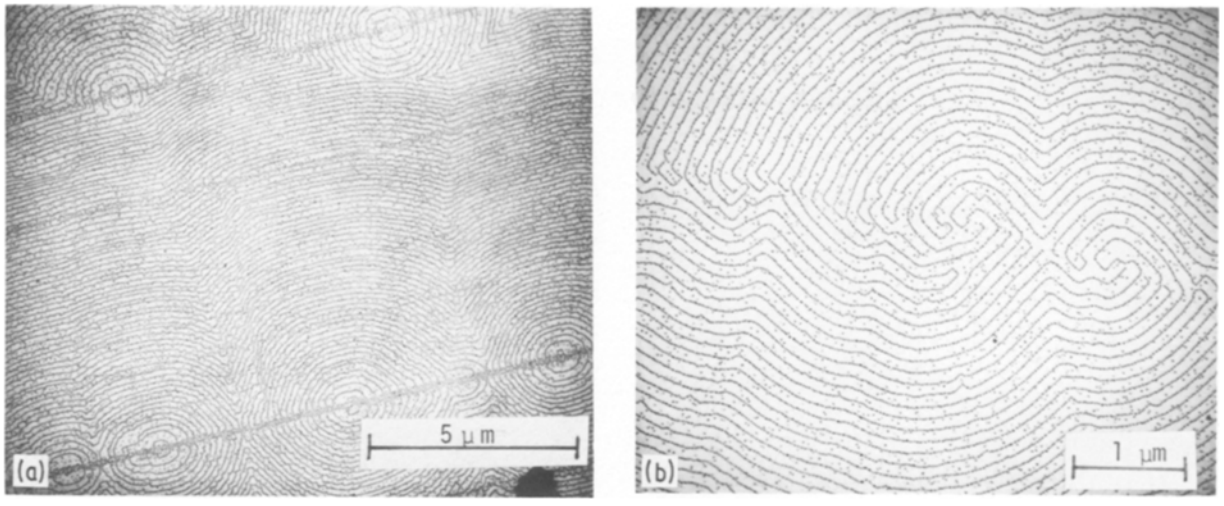

Figure 12 (a) Evaporation lamellae generated along a low angle tilt boundary. (b) Evaporation lamellae generated along a low angle twist boundary.

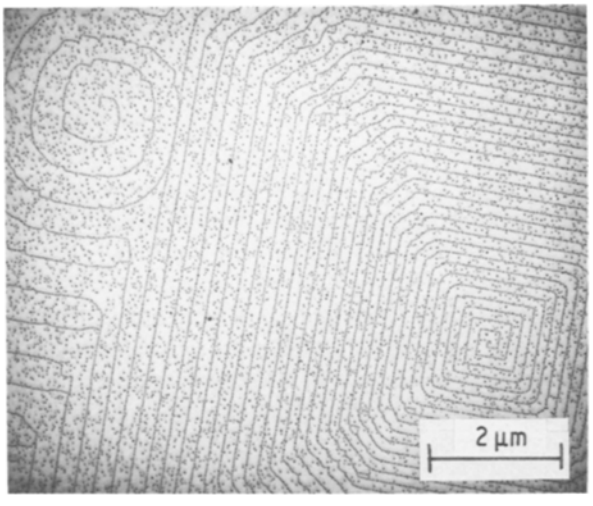

Figure 13 The splitting of a_0 high (square) steps into two $a_0/2$ high (round) steps on evaporated (1 0 0) surface of NaCl.

hand. It has been reported that thermal pits originate at points of emergence of dislocations [16, 17]. However, in other studies, it was concluded that thermal pits nucleation is dominated by surface impurities [18, 19]. In a recent study [11] it was observed that the nucleation and growth of thermal pits is enhanced by the presence of an externally applied electric field.

4. Step motion during evaporation

The displacement of ledges during the evaporation of alkali halides has been investigated primarily by two techniques. The first involves the use of the matching mirror surface (resulting from cleavage) as a reference to determine step displacements [20]. The second is the double decoration technique described earlier [5, 6]. Fig. 16 shows an example of the use of the latter technique to determine step displacements during the evaporation of sodium chloride [10].

During isothermal evaporation, the rate of displacement, i.e. velocity of a step, depends on its height and spacing relative to its neighbours [2]. Since the height of a square step (a_0) is twice that of a round step, the velocity of the former is expected to be half of that of the latter. A qualitative evidence for this theoretical expectation is demonstrated in Fig. 17. The effect of step separation, λ, on the step velocity has been treated theoretically by Burton *et al.* [2]. Neighbouring steps exert influence on each other when the diffusion fields of adatoms generated from the steps overlap. In

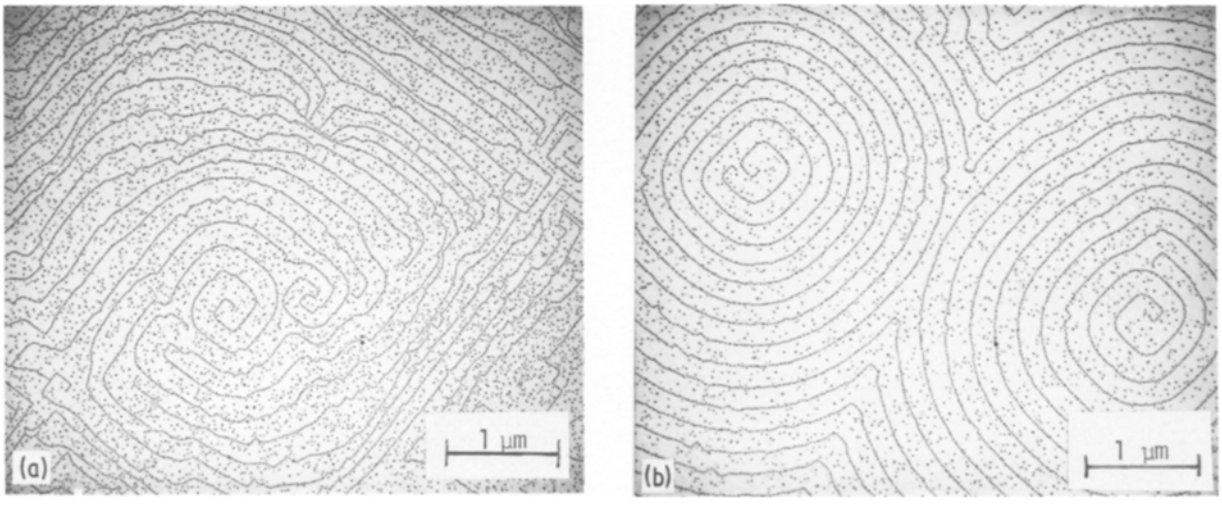

Figure 14 (a) The interaction of steps of screw dislocations with the same twist direction. (b) The interaction of steps of screw dislocations with opposite twist directions.

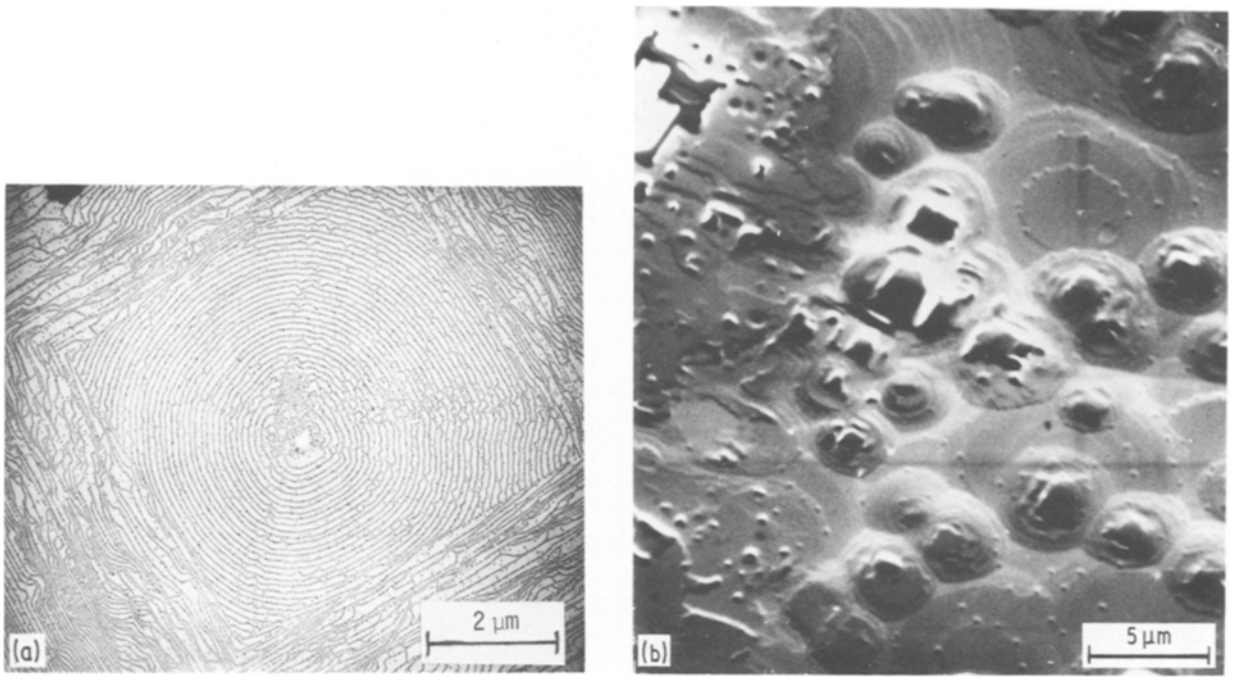

Figure 15 (a) Initiation of a thermal etch pit on evaporated (1 0 0) surface of NaCl. $T = 763$ K, $t = 30$ min. (b) High temperature thermal etch pits on evaporation (1 0 0) surface of KCl. $T = 793$ K, $t = 120$ min.

accordance with the BCF theory, the effect of λ on the velocity (v) of a step in a train of steps is given by

$$v = v_\infty \tanh (B\lambda) \quad (1)$$

where v_∞ is the step velocity at infinite step separation and B is defined by

$$B = (2^{1/2} X_s)^{-1} \quad (2)$$

with X_s being the surface self-diffusion length. Velocities measured for steps generated by screw dislocation are plotted in Fig. 18 against step separation for sodium chloride crystals evaporated at the indicated temperatures. Measurements made on edge dislocation steps gave similar results [5]. From the temperature dependence of v_∞, it is possible to calculate the activation energy for evaporation [5]. Calculations made for NaCl gave an activation energy of $228.1 \pm 7.3\,\text{kJ mol}^{-1}$ which compares favourably with values determined from recent thermogravimetric experiments [21, 22].

As indicated earlier in this paper, the nucleation of DSHs at any given location is influenced by the proximity of the site to surface steps since the latter act as sources of adatoms during evaporation. We have investigated the dependence of the nucleation of DSHs on the separation between the neighbouring steps, λ, in dislocation-generated evaporation lamellae during the evaporation of NaCl. The minimum values of step separation, λ_{min}, for which DSHs were observed are shown on the curves of Fig. 18. Also shown on these curves are values of v_∞ for the four experimental temperatures. With the exception of the low temperature data, the results show a good correspondence between λ_{min} and the step separation corresponding to v_∞. The step separation at which the velocity is independent of λ can be determined theoretically [2] as

$$\lambda_\infty = 3 \times 2^{1/2} X_s \simeq 4X_s \quad (3)$$

where λ_∞ is the step separation corresponding to v_∞

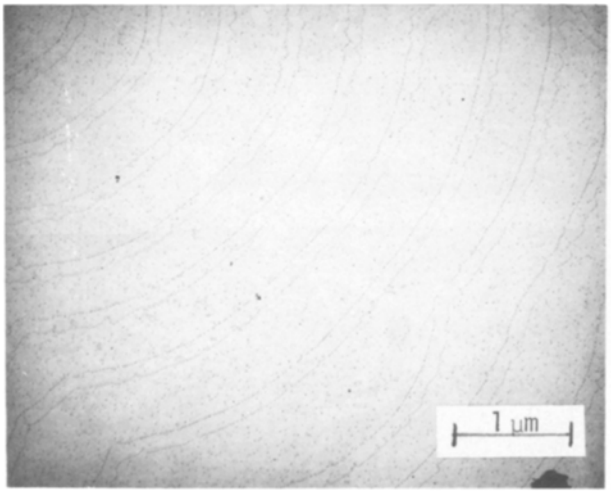

Figure 16 Displacement of surface steps during evaporation made visible by the double decoration technique.

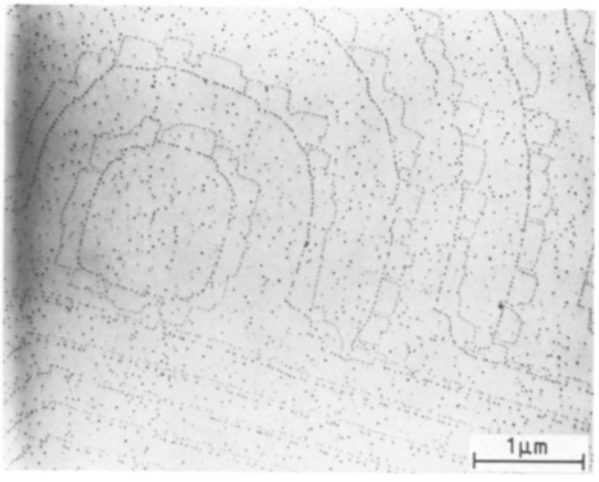

Figure 17 Relative displacements of a_0 and $a_0/2$ high steps during evaporation of a (1 0 0) surface of NaCl.

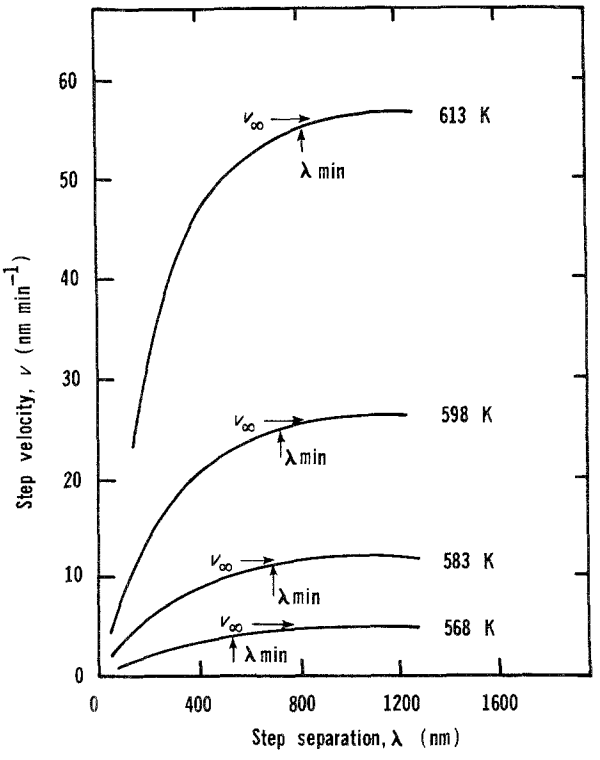

Figure 18 Dependence of step velocity on step separation for screw dislocation generated evaporation lamellae.

and X_s is the surface self-diffusion length. From step velocity measurements, reported elsewhere [5], X_s values have been calculated for edge and screw dislocation generated evaporation lamellae. In theory, therefore, at $\lambda = \lambda_\infty$ the diffusion fields of adatoms do not overlap and the nucleation of DSHs is possible. Thus, the values of λ_∞ calculated from X_s values are the theoretical λ_{min} values. Table I lists both observed and calculated λ_{min} for DSH nucleation on (1 0 0) surfaces of NaCl. Also listed in Table I are the values of X_s which were determined from measurement of velocities of screw dislocation-related steps [5]. In all cases the theoretically calculated λ_{min} values are higher than the observed values, although the difference between the two becomes smaller with increasing temperature. In an analogous experiment in which step velocities were determined during growth [8], a discrepancy (by a factor of 4 to 5) between calculated and observed λ_{min} values was noted and attributed to possible surface contamination.

TABLE I Calculated and observed minimum step separation for the nucleation of disc-shaped holes on (1 0 0) surfaces of NaCl

T (K)	X_s (nm)	λ_{min} (obs) (nm)	λ_{min} (calc) (nm)
568	329	654	1316
583	289	695	1156
598	257	736	1028
613	240	818	960

Straight ledges on cleaved (1 0 0) surfaces of alkali halides correspond to ⟨1 0 0⟩ directions. Thus when straight steps in square spirals or loops maintain their geometry as they move during evaporation, it is concluded that the motion of ⟨1 1 0⟩ ledges must be rapid relative to that of ⟨1 0 0⟩ steps. If this were not the case then the square geometry of an evaporation lamella would soon blunt at the corners and change into an octagonal pattern. Such patterns, however, are observed on initially square lamellae at locations far from the dislocation source. This observation has been attributed to the relative effect of impurities on the motion of ⟨1 1 0⟩ and ⟨1 0 0⟩ steps [4]. Steps having the ⟨1 1 0⟩ direction contain, per force, a higher concentration of kinks and hence are more likely to accumulate surface impurities. Thus the attachment of impurities to the ⟨1 1 0⟩ steps leads to a decrease in their velocity resulting in the geometry shown in Fig. 19. Another aspect of this phenomenon is provided by observations on step displacements using the double decoration technique. Fig. 20 shows that the movement of a round step is not isotropic with respect to crystalline directions. Portions of the steps which are initially aligned along the ⟨1 0 0⟩ directions move uniformly while those which are aligned approximately along the ⟨1 1 0⟩ directions move in a non-uniform manner. The displacement of the latter segments of the original step results in a stairs-like morphology, with straight segments oriented along ⟨1 0 0⟩ directions. Thus, movement of the step along ⟨1 1 0⟩ directions is possibly hindered by the presence of the gold particles

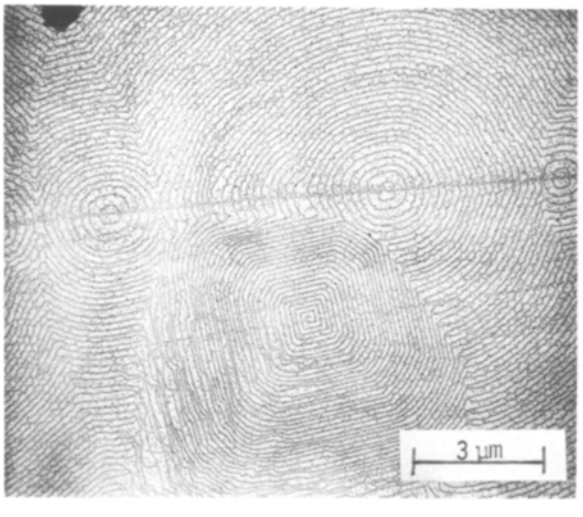

Figure 19 Polygonization of square lamellae suggesting retardation of advancements of steps along [1 1 0] directions.

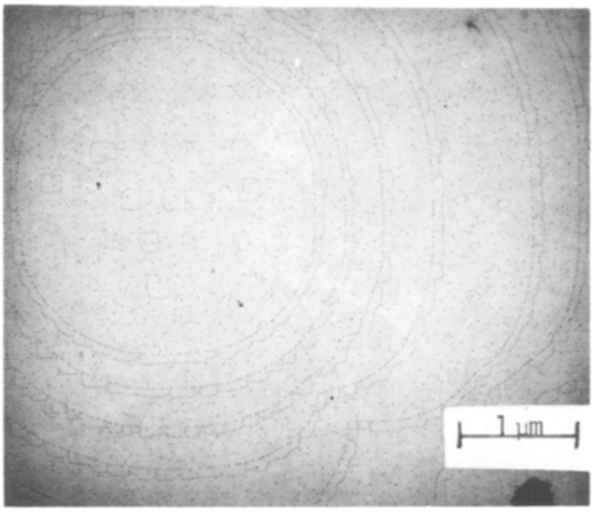

Figure 20 Anisotropic displacement of evaporation steps on cleaved (1 0 0) surfaces of NaCl.

from the first decoration or by adsorbed surface impurities. Since the morphology depicted in Fig. 20 was only observed in relatively few experiments, we conclude that the anisotropy of ledge movement is due to the preferred association of impurities with $\langle 1\,1\,0 \rangle$ segments of the steps. This conclusion is further supported by the fair agreement between velocities measured by the double decoration technique [5] and those determined by another method requiring only one decoration [23].

Acknowledgements

This work was supported by a grant from Ceramic and Electronic Materials Program (DMR-8404007), Division of Materials Research of the National Science Foundation.

References

1. J. P. HIRTH and G. M. POUND, *J. Chem. Phys.* **26** (1957) 1216.
2. W. K. BURTON, N. CABRERA and F. C. FRANK, *Phil. Trans. R. Soc. (Lond)* **A243** (1951) 299.
3. G. A. BASSETT, *Phil. Mag.* **3** (1958) 1042.
4. Z. A. MUNIR, E. K. CHIEH and J. P. HIRTH, *J. Cryst. Growth* **63** (1983) 244.
5. H. Z. DURUSOY and Z. A. MUNIR, *Phil. Mag.* **A52** (1985) 383.
6. K. W. KELLER, in "Crystal Growth and Characterization, edited by R. Ueda and J. B. Mullins (North-Holland, Amsterdam, 1985) p. 361.
7. J. L. ROBINS, T. N. RHODIN and R. L. GERLACH, *J. Appl. Phys.* **10** (1966) 3893.
8. H. BETHGE, in "Molecular Processes on Solid Surfaces", edited by E. Drouglis, R. D. Gertz and R. I. Jaffee (McGraw-Hill, New York, 1969).
9. G. VLASAK, *Acta Phys. Slovaca* **28** (1978) 166.
10. H. Z. DURUSOY, Ph.D. Thesis, University of California, Davis, California, 1984.
11. C. A. MACHIDA and Z. A. MUNIR, *J. Cryst. Growth* **68** (1984) 665.
12. K. W. KELLER, *Growth of Crystals* **7** (1969) 145.
13. T. SUREK, J. P. HIRTH and G. M. POUND, *J. Cryst. Growth* **18** (1973) 20.
14. G. TORRES, I. ALVAREZ and S. REYES, *Acta Cryst.* **A24** (1968) 685.
15. V. SUDHAKAR and I. V. I. BHAGAVAN RAJU, *Surf. Technol.* **16** (1982) 349.
16. A. R. PATEL, O. P. BAHL and A. S. VAGH, *Acta Cryst.* **19** (1965) 1025.
17. T. EJIMA, W. H. ROBINSON and J. P. HIRTH, *J. Cryst. Growth* **7** (1970) 155.
18. A. GRINBERG, *Surf. Sci.* **2** (1964) 314.
19. J. BUDKE, *J. Appl. Phys.* **40** (1969) 641.
20. H. BETHGE, K. W. KELLER and E. ZIEGLER, *J. Cryst. Growth* **3/4** (1968) 184.
21. R. H. WAGONER and J. P. HIRTH, *J. Chem. Phys.* **67** (1977) 3074.
22. Z. A. MUNIR and T. T. NGUYEN, *Phil. Mag.* **A47** (1983) 105.
23. H. HOCHE and H. BETHGE, *J. Cryst. Growth* **42** (1977) 110.

Received 11 August
and accepted 23 September 1986